

Photocoupling of $\text{Ag}_3\text{PO}_4\text{-Ag}_2\text{CO}_3$ with molecularly imprinted Polymer for enhanced removal of phenol under solar light: Application of Taguchi method

Hager R. Ali*

*Spectroscopic Division, Analysis and Evaluation Department,
Egyptian Petroleum Research Institute, 11727 Nasr City, Cairo, Egypt.*

**Corresponding author*

Abstract

In the current study, photocoupling of $\text{Ag}_3\text{PO}_4\text{-Ag}_2\text{CO}_3$ with molecularly imprinted Polymer was synthesized and characterized by XRD, FTIR and SEM analyses under sun light. The results suggested the application of the synthesized photocatalyst in photocatalytic degradation of phenol was studied using the Taguchi method and the chosen parameters were as follows: pH (2–9), concentration (50–300 mg/l), solar light radiation time (30–180 min), and catalyst dosage (0.5–3.5 g/l). The results indicate that the optimum dosage of the catalyst 1.5 g/l, pH = 9, phenol concentration = 50 mg/l, and irradiation time = 120 min, and the phenol removal efficiency reached up to 73.9 % at these optimal conditions.

Keywords: Molecularly imprinted Polymer, phenol, photocatalytic efficiency, $\text{Ag}_3\text{PO}_4\text{-Ag}_2\text{CO}_3$, heterogenous catalyst

INTRODUCTION

Molecular imprinting polymer (MIP) is a well-known technique to generate highly selective synthetic polymer receptors for target molecules. Recently, Multifunctional composite materials prepared from different functional elements have attracted great interest because of their many practical applications. Combining MIPs with inorganic nanoparticles can lead to new chemical sensors [1–3], high efficiency photocatalysts, [4,5] and magnetic adsorbents useful for fast molecular separation [6–8]. Because of their synthetic accessibility, molecularly imprinted polymer (MIP) is ideal building blocks for preparing multifunctional composites. Formation of a heterojunction (or interface) over two semiconductors has already proven to be an effective way to improve photocatalytic activity or stability, according to previous reports. Theoretically, when a p-type semiconductor and n-type semiconductor form a p–n junction, a strong inner electric field will be formed near the junction, pointing from n toward p, owing to the arrangement of the high concentrations of negatively and positively charged ions. The difference of the electric potential in the electric field can enhance the separation of photogenerated electrons and holes, increasing the quantum efficiency of the photocatalytic reactions [9–12]. The p–n

junction photocatalysts, have been shown to exhibit a high photocatalytic efficiency compared with other heterojunctions. Therefore, Ag_2CO_3 , as a p-type semiconductor, can form a p–n heterojunction with Ag_3PO_4 , which is an n-type semiconductor. Phenolic pollutants are toxic in nature. Their presence can be commonly observed in the streams of various industrial wastewaters [13, 14]. The presence of phenolic compounds represents a serious potential hazard for human health and aquatic life, and that is why phenols have been registered as a priority pollutant by the US Environmental Protection Agency (USEPA) [15] with a permissible limit of 0.1 mg/l in wastewater [15, 16]. In this work, we developed a general photocoupling chemistry to enable simple conjugation of MIP with inorganic catalyst. The photocatalytic activity of the material was evaluated by phenol degradation under solar light irradiation and different conditions.

EXPERIMENTAL SECTION

Photocatalyst synthesis of $\text{Ag}_3\text{PO}_4\text{-Ag}_2\text{CO}_3$

All chemicals were of analytical grade purity and used without further purification. Briefly, 252 mg NaHCO_3 and 312 mg $\text{NaH}_2\text{PO}_4 \cdot 2\text{H}_2\text{O}$ were dissolved in 80 mL deionized water under stirring. Then, 40 mL AgNO_3 aqueous solutions (approximately 0.3 mol/L) was added dropwise to the solution under stirring. The precipitate was collected by centrifugation, washed three times with deionized water after stirring for 12 h and dried in air at 70 °C for 12 h to yield the 40% $\text{-Ag}_3\text{PO}_4\text{-Ag}_2\text{CO}_3$ composite photocatalyst (40 mol% Ag_3PO_4 and 60 mol% Ag_2CO_3).

Preparation of molecular imprinted polymer (MIP/ $\text{Ag}_3\text{PO}_4\text{-Ag}_2\text{CO}_3$)

A typical procedure for preparing MIP is as following: 0.15 g phenol (1 mmol) and 0.12 g styrene were dissolved in 10 mL of dichloromethane with 0.1 g of dispersed $\text{Ag}_3\text{PO}_4\text{-Ag}_2\text{CO}_3$ and stirred for 4 hours. Then 2.93 g EGDMA and 0.122 g benzoyl peroxide were added to the solution under nitrogen atmosphere. After hyper acoustic mixing, the mixture was then polymerized overnight by thermal initiation at 80°C, free phenol in the

formed polymer was continuously extracted and washed with methanol/acetic acid solution (9:1, v/v) until no phenol was detected by HPLC Instrument, phenol free MIP was washed by water, dried overnight and kept for further investigation. The resultant polymer was coded as MIP/ Ag₃PO₄-Ag₂CO₃.

Design of experiments (DOE)

In order to photodegrade phenol, the Taguchi method, a powerful tool for design of experiments, were applied to determine the optimum number of the experiments [17]. This method has been used by other researchers for statistical analysis in advanced oxidation processes [18]. This technique includes data transformation to a signal-to-noise (S/N) ratio,

which is a measure of the variations presented, and the larger the S/N ratio, the more important the factors and the better the results [19]. In this paper for evaluating the performance of synthesized catalyst, determining optimum operational condition we used the Taguchi method in which initial pH value of the phenol solution, concentration, dosage of the catalyst, and irradiation time are considered as the effective parameters. The factors and their assigned levels are presented in Table (1). The photocatalytic experiments were performed using solutions of phenol at different initial pH values (2–9), concentrations (50–300 mg/l), solar light radiation time (30–180 min), and catalyst dosage (0.5–3.5 g/l).

Table 1: Factors and their levels for design of experiments

Variables		Levels			
		1	2	3	4
1	pH	2	5	7	9
2	Dose (g/l)	0.5	1.5	2.5	3.5
3	Conc.(mg/l)	50	100	250	300
4	Time (hr)	2	3	4	6

For analysis of the results and optimization of the conditions, Minitab software (Version 17) was used and the efficiency of

photocatalytic reaction was reported as % degradation.

Table 2: Experimental layout for using the L16OA and experimental result for phenol removal

Run No.	pH	Dose g/l	Conc. mg/l	Time hr	%degradation	S/N ratio
1	2	0.5	50	2	70.00	36.9020
2	2	1.5	100	3	68.78	36.7492
3	2	2.5	250	4	71.78	37.1201
4	2	3.5	300	6	67.00	36.5215
5	5	0.5	100	4	71.90	37.1346
6	5	1.5	50	6	70.00	36.9020
7	5	2.5	300	2	68.00	36.6502
8	5	3.5	250	3	67.00	36.5215
9	7	0.5	250	6	67.80	36.6246
10	7	1.5	300	4	69.00	36.7770
11	7	2.5	50	3	71.94	37.1394
12	7	3.5	100	2	70.40	36.9515
13	9	0.5	300	3	69.00	36.7770
14	9	1.5	250	2	73.9	37.3729
15	9	2.5	100	6	68.90	36.7644
16	9	3.5	50	4	69.00	36.7770

For each experiment, a solution of the phenol with desired concentration was prepared, and after adjusting the pH value, it was injected into the reactor chamber along with the needed dosage of the catalyst (according to the Taguchi table). The pH of the solution was adjusted on desired values using HCl and NaOH diluted solutions with the aid of pH meter. After the reaction period was over, the resulting solution was analyzed by the HPLC. In order to monitor the phenol concentration, samples of the solution were taken out of the reactor after the reaction time and the photocatalyst particles were filtered and separated after a 10 min centrifugation process at 5000 rpm in a centrifuge. The degree of photodegradation (efficiency) as a function of time, which demonstrates the efficiency of the experiment, could be calculated with the following equation:

$$RE = \left(\frac{C_o - C_e}{C_o} \right) \times 100 \quad (1)$$

Where C_o and C_e (mg/l) are the initial and final phenol concentrations, respectively.

RESULTS AND DISCUSSION

Characterization of the catalyst

The crystallographic structures of the as-prepared samples were examined by X-ray powder diffraction (XRD). As shown in Fig (1) X-ray of the $Ag_3PO_4-Ag_2CO_3$ samples. The peaks at 18.5° (020), 20.6° (110), 32.6° (-101), 33.7° (-130), 37.1° (040) and 39.6° (031) are indexed to that of monoclinic Ag_2CO_3 (JCPDS 01-073-4385). Further, the crystallite size was calculated using Scherrer's formula for the high intensity peak, the estimated grain size was found to be 87 nm with d-spacing 0.227 nm. The peaks at 21.0° (110), 29.8° (200), 33.4° (210), 36.7° (211), 47.9° (310), 52.8° (222), 55.1° (320) and 57.4° (321) are indexed to that of cubic Ag_3PO_4 (JCPDS 00-006-0505), the estimated grain size was found to be 81.95 nm with d-spacing 0.16 nm., the diffraction peaks of both Ag_3PO_4 and Ag_2CO_3 can be observed in the MIP/ $Ag_3PO_4-Ag_2CO_3$ composite polymer samples but with low intensity compared to the catalyst alone.

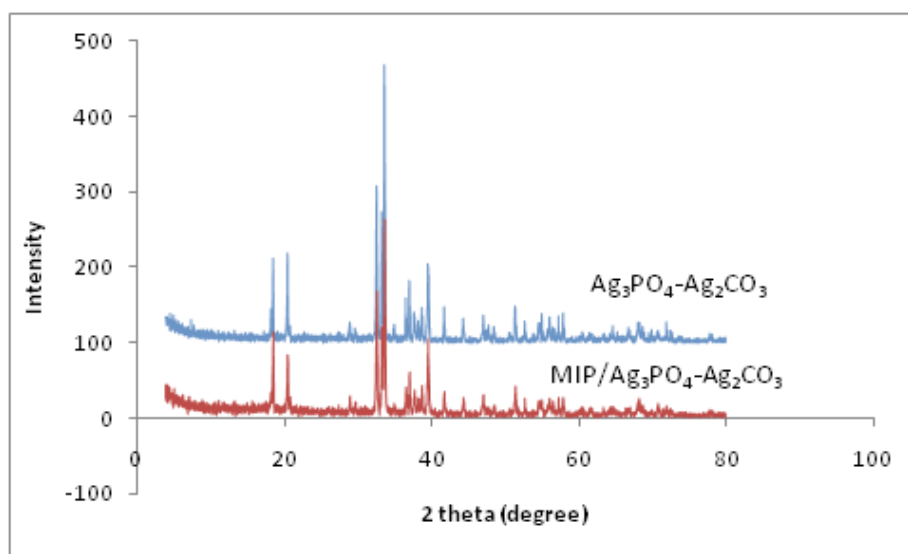


Figure 1: XRD patterns of prepared catalyst

In FT-IR spectrum of $Ag_3PO_4-Ag_2CO_3$ Fig (2) absorption peaks at 567 and 1016 cm^{-1} can be attributed to the stretching vibrations of the PO_4 group [20] which verify the existence of Ag_3PO_4 in the sample, and the peaks around 1600 and 3200 cm^{-1} represent the physically adsorbed water on the catalyst surface. The characteristic absorption bands of CO_3^{2-} could be observed at 708 cm^{-1} , 802 cm^{-1} , 883 cm^{-1} , 1328 cm^{-1} and 1449 cm^{-1} [21]. Besides, the peaks at 1640 cm^{-1} and 1540 cm^{-1} are found and the peak intention of CO_3^{2-} . The IR peaks at 1140 and 1730 cm^{-1} corresponds to C-O and C=O in EGDMA, respectively in case of MIP/ $Ag_3PO_4-Ag_2CO_3$. The original cross-linking agent EGDMA and styrene have abundant vinyl

groups. However, the characteristic C=C peaks at 1630 , 990 , and 910 cm^{-1} show low intensity that verified the crosslinking polymerization reaction. After surface grafting, a new vibrational peak appears in the polymer sample around $2990-2995\text{ cm}^{-1}$ belongs to aliphatic C-H stretching vibration. Additionally, flexions at $700-1000\text{ cm}^{-1}$ corresponding to aromatic C-H bond can be seen in the spectra. Peaks observed at 1313 , 1185 and 1046 cm^{-1} related to the =C-H in-plane vibration and the =C-H out-of-plane vibration is found at 617 and 918 cm^{-1} . Data strongly confirms the formation hydrogen-bonding interactions between imprinted polymer and phenol molecule.

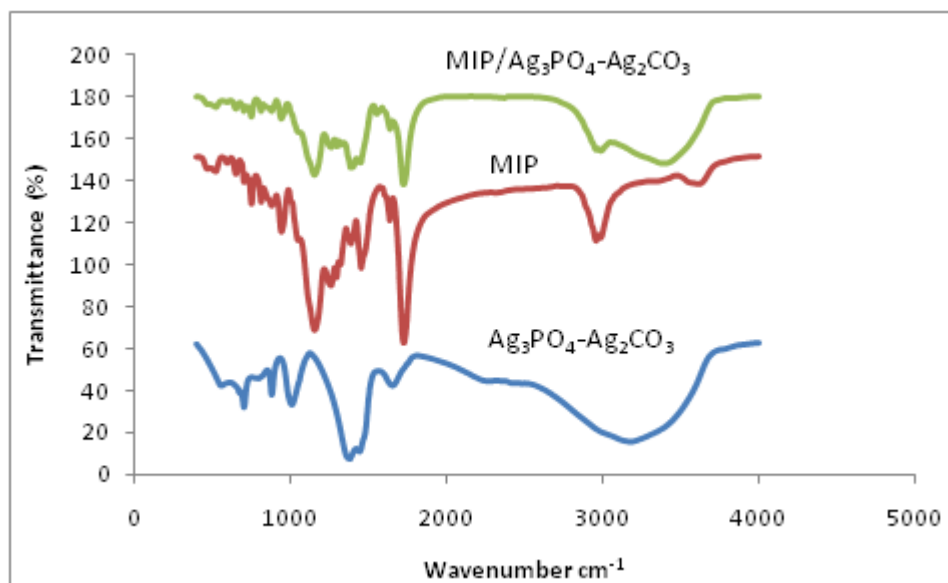


Figure 2: FTIR curves of the prepared materials

Formation of specific cavities into polymer matrix loaded with $\text{Ag}_3\text{PO}_4\text{-Ag}_2\text{CO}_3$ plays an important role in the selective reorganization and photodegradation of phenol. The surface morphology of free and loaded polymer was examined using scanning electron microscopy. SEM images Fig. 3 (A) show particles with a polyhedral morphology similar to rhombic

dodecahedral particles of $\text{Ag}_3\text{PO}_4\text{-Ag}_2\text{CO}_3$. Irregular shapes were found in the prepared molecular imprinting material (MIP) Fig. 3 (B) has abundant pores on the coarse surface with $\text{Ag}_3\text{PO}_4\text{-Ag}_2\text{CO}_3$ deposited on the surface of polymer Fig. 3 (C).

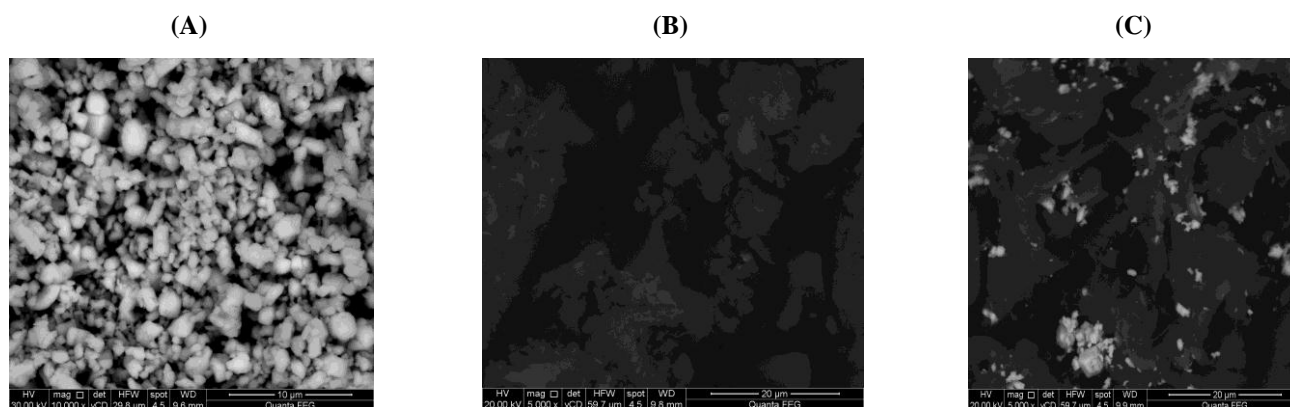


Figure 3: SEM images of (A) $\text{Ag}_3\text{PO}_4\text{-Ag}_2\text{CO}_3$ (B) IMP (C) IMP/ $\text{Ag}_3\text{PO}_4\text{-Ag}_2\text{CO}_3$

Photocatalytic activity

Taguchi orthogonal array L_{16} shows the effect of pH, dose, concentration and time on the photocatalytic activity of $\text{Ag}_3\text{PO}_4\text{-Ag}_2\text{CO}_3$ on to imprinted polymer using simulated sunlight irradiation for phenol degradation. Solar irradiation plays an important role in the photocatalytic process in order to generate hydroxyl radicals, the removal efficiency of phenol was recorded only 10% without

exposure to the solar irradiation. The removal of phenol was due to the adsorption mechanism on the surface of $\text{Ag}_3\text{PO}_4\text{-Ag}_2\text{CO}_3$ and beside the cavity of polymer.

The obtained results after elapsing the desired irradiation time are presented in Table (2). The optimum value for each parameter was as follows: pH = 9, phenol concentration = 50 mg/l, catalyst dosage = 1.5g/l and solar light time = 120 min.

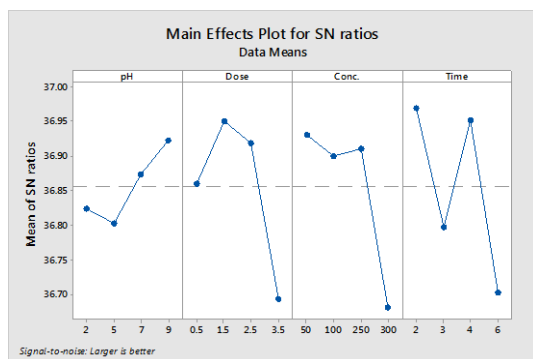


Figure 4: Response table for mean S/N ratios of MIP/Ag₃PO₄-Ag₂CO₃ for phenol degradation

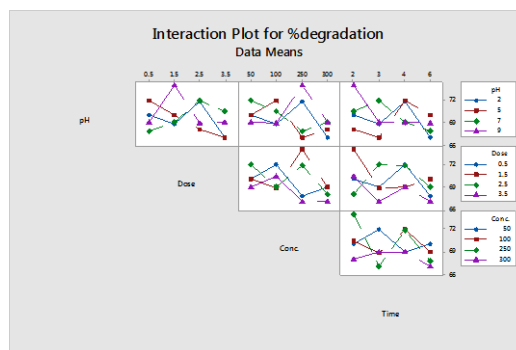


Figure 5: Interaction plot of MIP/Ag₃PO₄-Ag₂CO₃ for phenol degradation

The initial concentration of organic pollutants in contaminated water is a significant parameter that affects the efficiency of the treatment process [23]. Results also show that as the initial phenol concentration was increased from 50 to 300 mg/L, the degradation efficiency decreased, this phenomenon is due to the decrease in the relative ratio of the hydroxyl radicals to the molecules of the organic contaminants in the solution as suggested by Hashim et al. [24]. They further stated that when the concentration of the pollutant increases, the amount of the molecule adsorbed onto the surface of the catalyst also increases resulting in fewer cavities bind with the recognition sites. Also, as the concentration of the compound increases, the solution becomes more turbid thereby reducing the amount of photons that get to the catalyst surface and as a result, the amount of hydroxyl radicals attacking the organic molecules becomes limited thus reducing the degradation efficiency [25, 26].

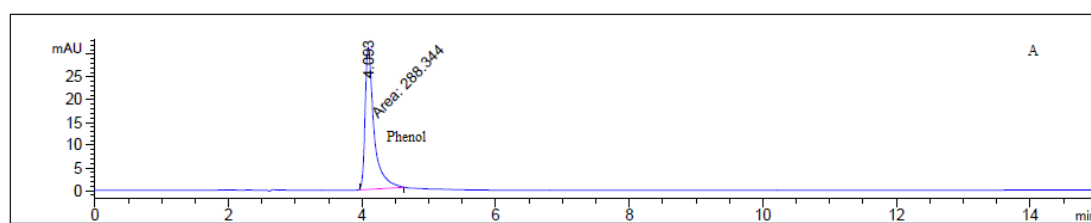
Fig(4) and confirmed by severe interaction between these factors as shown in Fig (5) shows the effect of catalyst loading on the photodegradation process. The results show that the percentage of phenol degraded increased with increasing catalyst loading up to 1.5g/L of MIP/Ag₃PO₄-Ag₂CO₃ and thereafter decreased with increasing MIP/Ag₃PO₄-Ag₂CO₃ loading. The decrease in degradation efficiency observed beyond a catalyst loading of 1.5 g/L could be attributed to the increase in the turbidity of the solution as a result of the excess catalyst present in the degradation reaction vessel. This leads to the so called screening effect that involves the reflectance, interception and scattering of light and hence a fraction of the available light rays do not penetrate into the solution [29]. A similar behavior was observed by

Hashim et al. [24] who reported that in batch or dynamic flow photoreactors, the initial reaction rates are directly proportional to the catalyst loading indicating a true heterogeneous catalytic regime, but above a certain loading limit, the reaction rate levels off and further increase in catalyst loading does not benefit the process. So et al. [30] suggested that agglomeration and sedimentation of the catalyst particles at high catalyst loading could also be responsible for the decrease in degradation efficiency.

During optimization of the removal of phenol, all factors affecting the activity of should be considered, particularly pH which is the most important factor, the concentration of free phenoxide ions and OH⁻ is expected to increase as solution becomes more basic. It is evident from the Fig. (4) That removal of phenol by MIP/Ag₃PO₄-Ag₂CO₃ was lower at acidic pH, due to pH below 7, a significantly high electrostatic attraction exists between the positively charged surface and phenolate ion (C₆H₅O⁻) similar observation was reported by Nabais et al, [22].

The optimum contact time is 120 min under sunlight recorded 73.9 % removal. It is reasonable to assume that the surface of MIP/Ag₃PO₄-Ag₂CO₃ has much imprinted cavities, the template phenol was easy to enter into the cavities and bind with the recognition sites. When the recognition sites were filled up, the rate of adsorption dropped significantly and adsorption process achieved equilibrium gradually.

Phenol oxidation process is accompanied with evolution of several aromatic intermediates, data obtained from high performance liquid chromatography Fig (6) show benzoquinone, hydroquinone, catechol and phenol.



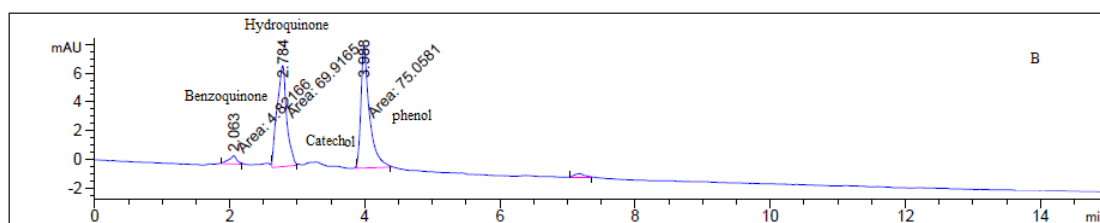


Figure 6: HPLC chromatogram of phenol (a) before and (b) after degradation under sunlight.

Implementation of ANOVA

In order to conduct an analysis of the relative importance of each factor more systematically, an ANOVA was applied to the data. The main objective of ANOVA is to extract from the results how much variations each factor causes relative to the total variation observed in the result [32]. The results of ANOVA are listed in Table (3), degree of freedom for the error is 3. According to the results, the F-ratio (0.11) for pH

is smaller than the F-Ratio for dose (0.49), concentration (0.51 and time (0.61). This means that the variance in pH is insignificant compared with the variance in dose and concentration that has a significant effect on the responses. Quantitative evaluation can be achieved using percentage contribution (P%) [33]. Percent contributions of all factors are presented in Table (3). The order of importance of factors is as follows: Time>Concentration > dose > pH.

Table3: ANNOVA Table

Source	Degree of freedom	Sum of squares	Mean of squares	F-value	P-value	Percentage contribution =ss/ss(tota)*100
pH	3	2.276	0.7586	0.11	0.949	3.8
Dose	3	10.154	3.3847	0.49	0.715	18
Concentration	3	10.569	3.5229	0.51	0.704	18.7
Time	3	12.680	4.2267	0.61	0.653	22.48
Error	3	20.812	6.9372			
Total	15	56.390				

CONCLUSIONS

In this research, application of photocoupling of Ag_3PO_4 - Ag_2CO_3 with molecularly imprinted polymer (MIP/ Ag_3PO_4 - Ag_2CO_3) for enhanced removal of phenol under solar light was investigated. The results indicate that the phenol concentration, pH, dose and solar light radiation time are respectively the most effective factors in these experiments. Considering the efficiency of the degradation process was significantly high even by using small quantities of this photocatalyst. With regard to the above-mentioned facts this method can be assumed as an applicable way to remove phenol from wastewaters.

ACKNOWLEDGEMENT

I have gratefully acknowledged for greatest support by Egyptian petroleum research institute (EPRI) for permission to collect literature from the library and their cooperation.

REFERENCES

- [1] Zhao Y, Ma Y, Li H, Wang L. Anal. Chem. 2012;84:386–395. [PubMed]
- [2] Matsui J, Akamatsu K, Nishiguchi S, Miyoshi D, Nawafune H, Tamaki K, Sugimoto N. Anal. Chem. 2004;76:1310–1315. [PubMed]
- [3] Tokonami S, Shiigi H, Nagaoka T. Anal. Chim. Acta. 2009;641:7–13. [PubMed]
- [4] Xu L, Pan J, Xia Q, Shi F, Dai J, Wei X, Yan Y. J. Phys. Chem. C. 2012;116:25309–25318.
- [5] Zhang W, Li Y, Wang Q, Wang C, Wang P, Mao K. Environ. Sci. Pollut. Res. Int. 2013;20:1431–1440. [PubMed]
- [6] Gonzato C, Courty M, Pasetto P, Haupt K. Adv. Funct. Mater. 2011;21:3947–3953.
- [7] Liu Y, Huang Y, Liu J, Wang W, Liu G, Zhao R. J. Chromatogr. A. 2012;1246:15–21. [PubMed]
- [8] Lu C-H, Wang Y, Li Y, Yang H-H, Chen X, Wang

- X-R. J. Mater. Chem. 2009;19:1077–1079.
- [9] Yu C L, Zhou W Q, Yu J C, Liu H, Wei L F. *Chin J Catal.* 2014, 35: 1609
- [10] Wang H L, Zhang L S, Chen Z G, Hu J Q, Li S J, Wang Z H, Liu J S, Wang X C. *Chem. Soc. Rev.* 2014, 43, 5234
- [11] Moniz S J A, Shevlin S A, Martin D J, Guo Z X, Tang J W. *Energy Environ Sci*, 2015, 8: 731
- [12] Zhang J S, Zhang M W, Sun R Q, Wang X C. *Angew Chem. Int. Ed.* 2012, 51: 10145
- [13] Cao S, Chen G, Hu X, Yue PL (2003) Catalytic wet air oxidation of wastewater containing ammonia and phenol over activated carbon supported Pt catalysts. *Catalysis Today* 88:37–47
- [14] Jiang H, Fang Y, Fu Y, Guo QX (2003) Studies on the extraction of phenol in wastewater. *J Hazard Mater B* 101:179–190
- [15] United States Environmental Protection Agency (USEPA) (1985) Technical support document for water quality based toxics control: EPA/440/485032. USEPA, Washington, DC
- [16] Srivastava VC, Swamy MS, Mall ID, Prasad B, Mishra IM (2006) Adsorptive removal of phenol by bagasse fly ash and activated carbon: equilibrium, kinetics and thermodynamics. *Colloid Surf A* 272:89–104
- [17] G. Taguchi, Introduction to Quality Engineering: Designing Quality into Products and Processes, Asian Productivity Organization, Tokyo, 1986.
- [18] J. Zolgharnein, N. Asanjrani, M. Bagtash, G. Azimi, Multi-response optimization using Taguchi design and principle component analysis for removing binary mixture of alizarin red and alizarin yellow from aqueous solution by nano γ -alumina, *Spectrochim. Acta, Part A* 126 (2014) 291–300.
- [19] Z. BerilGönder, Y. Kaya, I. Vergili, H. Barlas, Optimization of filtration conditions for CIP wastewater treatment by nanofiltration process using Taguchi approach, *Sep. Purif. Technol.* 70 (2010) 265–273.
- [20] N. Mohaghegh, E. Rahimi and M. R. Gholami, *Mater. Sci. Semicond. Process.*, 2015, 39, 506–514.
- [21] Y. X. Song, J. X. Zhu, H. Xu, C. Wang, Y. G. Xu, H. Y. Ji, K. Wang, Q. Zhang and H. M. Li, *J. Alloys Compd.*, 2014, 592, 258–265.
- [22] Nabais, J.M.V., Suhas J.A.G., Carrott, Laginhas, P.J.M., and Roman, C., S., Phenol removal onto novel activated carbons made from lignocellulosic precursors: influence of surface properties, *J. Hazard. Mater.*, (2009), vol. 16, pp: 904–910.
- [23] Hong, S.S.; Ju, C.S.; Lim, C.G.; Ahn, B.H.; Lim, K.T.; and Lee, G.D. (2001). A photocatalytic degradation of phenol over TiO₂ prepared by sol-gel method. *Journal of Industrial and Engineering Chemistry*, 7(2), 99-104.
- [24] Hashim, H.A.A.; Mohamed, A.R.; and Lee, K.T. (2012). Solar photocatalytic degradation of tartrazine using titanium dioxide. *Jurnal Teknologi*, 35(1), 31-40.
- [25] Akyol, A.; Yatmaz, H.C.; and Bayramoglu, M. (2004). Photocatalytic decolorization of remazol red RR in aqueous ZnO suspensions. *Applied Catalysis B: Environmental*, 54(1), 19-24.
- [26] Byrappa, K.; Subramani, A.K.; Ananda, S.; Rai, K.L.; Dinesh, R.; and Yoshimura, M. (2006). Photocatalytic degradation of rhodamine B dye using hydrothermally synthesized ZnO. *Bulletin of Materials Science*, 29(5), 433-438.
- [27] Akpan, U.G.; and Hameed, B.H. (2009). Parameters affecting the photocatalytic degradation of dyes using TiO₂-based photocatalysts: A review. *Journal of Hazardous Materials*, 170(2-3), 520-529.
- [28] Inamdar, J.; and Singh, S.K. (2008). Photocatalytic detoxification method for zero effluent discharge in dairy industry: Effect of operational parameters. *International Journal of Chemical and Biological Engineering*, 1(4), 160-164.
- [29] Saquib, M.; Tariqa, M.A.; Faisala, M.; and Muneer, M. (2008). Photocatalytic degradation of two selected dye derivatives in aqueous suspensions of titanium dioxide. *Desalination*, 219(1-3), 301-311.
- [30] So, C.M.; Cheng, M.Y.; Yu, J.C.; and Wong, P.K. (2002). Degradation of azo dye procion red MX-5B by photocatalytic oxidation. *Chemosphere*, 46(6), 905-912.
- [31] E.E. Bamuza-pemu, E.M.N. Chirwa, "Profile of Aromatic Intermediates of Titanium Dioxide Mediated Degradation of Phenol," *Chem. Eng. Trans.* vol.35, pp. 1333–1338, 2013.
- [32] J. Latimer, J. Zheng. The sources, transport, and fate of PAH in the marine environment P.E.T. Douben (Ed.), PAHs: an ecotoxicological perspective, John Wiley and Sons Ltd, New York (2003)
- [33] Roy, R.K., 1990. A primer on the Taguchi method. Van Nostrand Reinhold, New York, USA, ISBN:13-9780442237295, pages: 247